

grid noise predictions. This may not be true when it comes to incorporating the nonaxisymmetric nozzle geometry and sound/flow interaction where the mean flow gradients dominate the whole mechanism of sound radiation. Accurate prediction of the flow-field including the shock structure is more important in properly estimating the shock-associated noise.

References

- ¹Mani, R., Balsa, T. E., Gliebe, P. R., Kantola, R. A., Stringes, E. J., and Wang, J. F. C., "High Velocity Jet Noise Source Location and Reduction," Task 2, Federal Aviation Administration, FAA-RD-76-79-II, Washington, DC, May 1978.
- ²Reichardt, H., "On a New Theory of Free Turbulence," *Royal Aeronautical Society Journal*, Vol. 47, June 1943, pp. 167-176.
- ³Khavaran, A., Krejsa, E. A., and Kim, C. M., "Computation of Supersonic Jet Mixing Noise for an Axisymmetric CD Nozzle Using $k-\epsilon$ Turbulence Model," AIAA Paper 92-0500, Jan. 1992.
- ⁴Cooper, G. K., and Sirbaugh, J. R., "PARC Code: Theory and Usage," Arnold Engineering Development Center, AEDC-TR-89-15, Tullahoma, TN, Nov. 1989.
- ⁵Chien, K. Y., "Prediction of Channel and Boundary Layer Flows with a Low Reynolds-Number Turbulence Model," *AIAA Journal*, Vol. 20, No. 1, 1982, pp. 33-38.
- ⁶Yamamoto, K., Brausch, J. F., Janardan, B. A., Hoerst, D. J., Price, A. O., and Knott, P. R., "Experimental Investigation of Shock-Cell Noise Reduction for Single Stream Nozzles in Simulated Flight Comprehensive Data Report," NASA CR-168234, May 1984.

Diverging Solutions of the Boundary-Layer Equations near a Plane of Symmetry

Hans Thomann*

Swiss Federal Institute of Technology,
8092 Zurich, Switzerland

Introduction

EXPERIMENTS with converging and diverging turbulent boundary layers near a plane of symmetry are described by Pompeo et al.¹ The test section used to generate the boundary layers on the plane $y = 0$ is shown in Fig. 1. The experiments were compared with computations based on a finite-difference boundary-layer code by Bettelini.² The prediction of the diverging flow agreed fairly well with the measurements and posed no special problems. The prediction of the converging flow, on the other hand, was very difficult. The results were very sensitive to the choice of parameters, and diverging solutions were observed for some combinations of parameters. It is the purpose of the present paper to investigate this tendency with different methods. Cases 1 and 2 are based on integral methods for laminar flow as described by Eichelbrenner.³ In case 1 the crossflow satisfies only the corresponding boundary condition at the wall which leads to a simple equation for the growth of the boundary-layer thickness. In case 2 the crossflow momentum equation is also taken into account, and case 3 uses Bettelini's code.² All three methods show that there exists a critical crossflow intensity beyond which the boundary-layer thickness $\delta(x)$ diverges at some x_s in the test section, and the same holds true also for turbulent flow. The results of case 1 and case 2 show that the skin friction vanishes at x_s . This divergence can, therefore, be called separation. However, it is a very peculiar case as no pressure gradient exists that could decelerate the x component of the flow. A similar situation exists in the plane of symmetry of a cone at angle of attack. Moore⁴ observed that the diverging flow on the windward side of cone posed no problems

whereas the converging flow on the leeward side became undetermined before separation of the crossflow took place. Boericke⁵ observed similar problems when using a finite-difference code. The flow on the leeward side of a blunted cone, as investigated by Der,⁶ is very similar to the present case. "Separation" is observed in both cases in spite of a vanishing axial pressure gradient. Good surveys of the state of the art are given by Refs. 3 and 7-9.

Assumptions and Equations

The external velocity field near the plane of symmetry ($z = 0$) was based on experiments of Pompeo et al.,¹ namely, $w_e(x, \delta, z) = w_z(x) \cdot z$ and $u_e(x, \delta, z) = U + w_{zx}(x) \cdot z^2/2$ with

$$w_z(x) = A \cdot \exp[(x - x_0)^2/B] \quad w_{zx} = \frac{dw_z}{dx}$$

For the converging flow good approximations are $A = -31.4 \text{ s}^{-1}$, $B = 0.231 \text{ m}^2$, and $x_0 = 1 \text{ m}$. The boundary layer was assumed to start at $x = -0.5 \text{ m}$ and to end at $x = 2.5 \text{ m}$. Figure 7 in Pompeo et al.¹ and w_z are comparable.

The velocity components near the plane of symmetry can be written as

$$u = u_0(x, y) + u_1(x, y) \cdot z + \dots$$

$$v = v_0(x, y) + v_1(x, y) \cdot z + \dots$$

$$w = w_1(x, y) \cdot z + \dots$$

Introducing these equations into the boundary-layer equations leads to the following expressions valid in the plane of symmetry near $z = 0$.

$$\frac{\partial u_0}{\partial x} + \frac{\partial v_0}{\partial y} + w_1 = 0 \quad (1)$$

$$u_0 \frac{\partial u_0}{\partial x} + v_0 \frac{\partial u_0}{\partial y} - v \frac{\partial^2 u_0}{\partial y^2} = 0 \quad (2)$$

$$u_0 \frac{\partial w_1}{\partial x} + v_0 \frac{\partial w_1}{\partial y} + w_1^2 - v \frac{\partial^2 w_1}{\partial y^2} = U w_{zx} + w_z^2 = S(x) \quad (3)$$

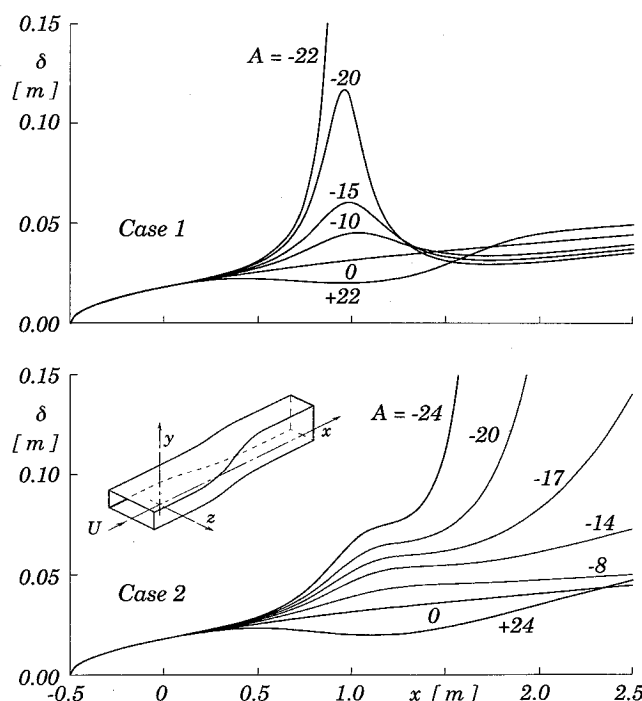


Fig. 1 Test section and boundary-layer thickness $\delta(x)$.

Received Jan. 24, 1994; revision received April 8, 1994; accepted for publication April 11, 1994. Copyright © 1994 by the American Institute of Aeronautics and Astronautics, Inc. All rights reserved.

*Professor, Department of Mechanical Engineering.

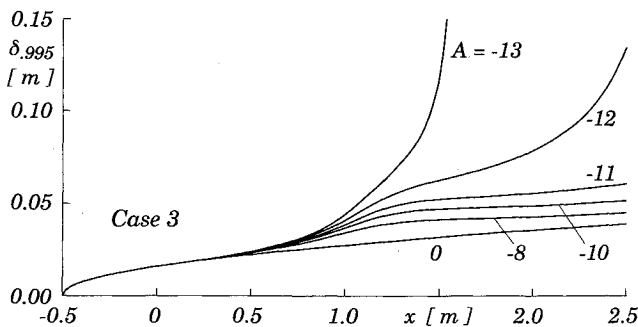
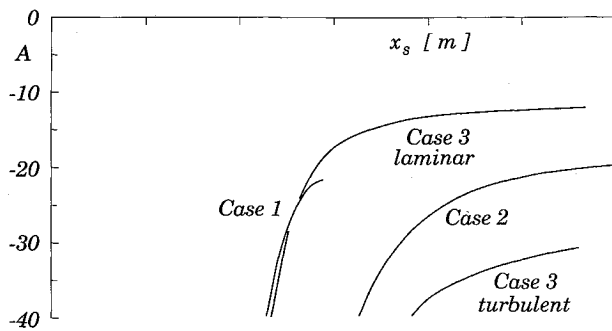
Fig. 2a Case 3 $\delta(x)$.

Fig. 2b Location of the singularity in the test section.

where $\nu = 8 \times 10^{-4} \text{ m}^2/\text{s}$ was chosen as this resulted in a boundary-layer thickness of 36 mm at $x = 1.5 \text{ m}$, which is typical for the experiment with two-dimensional flow. At $y = \delta$ the boundary conditions are $u_0 = U = 42 \text{ m/s}$ and $w_1 = w_z(x)$.

Integral Methods

In this classical approach (e.g., Schlichting¹⁰) velocity profiles are chosen for u_0 and w_1 ; v_0 is eliminated with the help of Eq. (1), and Eq. (2) is integrated from $y = 0$ to δ . The Pohlhausen profile for constant $u_e = U$ was chosen as $u_0 = U f(\eta)$ with $f(\eta) = 2\eta - 2\eta^3 + \eta^4$ and $\eta = y/\delta$.

Case 1

In this case the crossflow w_1 was also based on a polynomial of fourth degree which satisfies Eq. (3) at the wall. The result is $w_1 = w_z f(\eta) + \delta^2 S(x) g(\eta)/6\nu$ with $g(\eta) = \eta - 3\eta^2 + 3\eta^3 - \eta^4$.

Two remarks have to be made. First, it is assumed that both the u and w profiles extend to the same distance δ from the wall. This is reasonable as it is the u defect that drives the crossflow in a curved flow. Second, w_1 depends only on local quantities and does not take into account the upstream history inherent in the momentum equation. This assumption is much more severe, but it does not change the general conclusions as a comparison with the results of case 2 and of the finite-difference code shows. Introducing u_0 and w_1 into the integrated form of Eq. (2) leads to, with $q = \delta^2$,

$$\frac{dq}{dx} = \frac{2f'(0)}{J_1 - J_3} \frac{\nu}{U} - 2 \frac{w_z}{U} q - \frac{J_2 - J_4}{3(J_1 - J_3)} \frac{S(x)}{\nu U} q^2 \quad (4)$$

Here

$$f'(0) = \frac{df}{d\eta}(\eta=0) = 2, \quad J_i = \int_0^1 h_i d\eta$$

with $h_1 = f$, $h_2 = g$, $h_3 = f^2$, and $h_4 = fg$.

Equation (4) was integrated with $q(x = -0.5) = 0$ for different crossflow parameters A using fourth-order Runge-Kutta. Results are shown in Fig. 1. The obvious influence of lateral divergence ($A > 0$) or convergence ($A < 0$) on q and thus δ is determined by the term with w_z in Eq. (4). More important in the present case is the contribution due to w_{zx} in $S(x)$. It takes into account the secondary flow induced by the curvature of the external streamlines. For con-

verging flow this secondary flow is directed toward the plane of symmetry for $x < 1$ which leads to the rapid growth of $\delta(x)$. As the crossflow grows with δ^2 and as δ grows with increasing crossflow, a singularity can occur at some $x_s < 1$ for $A < -22$.

With the numbers appropriate to the experiment the last term in Eq. (4) dominates close to x_s , and Eq. (4) can be approximated with $dq/dx = p(x)q^2$. Starting with a given $q_1(x_1)$ the solution becomes

$$\frac{1}{q(x)} = \frac{1}{q_1} - \int_{x_1}^x p(x) dx$$

Sufficiently negative w_{zx} lead to $p(x) > 0$ which results in $1/q = 0$ at some x_s and thus to the singularity of δ . The skin friction will vanish at x_s as it is proportional to $1/\delta$.

Case 2

To take into account the upstream history of the crossflow, the corresponding profile was extended, following Eichelbrenner,³ to $w_1 = w_z f(\eta) + 2rg(\eta) + 6(r-s)\eta g(\eta)$ with $s = qS/12\nu$. An additional equation $dr/dx = fn(x, q, r, A)$ was derived with lengthy algebra from the integrated form of Eq. (3). The equation corresponding to Eq. (4) was integrated as for case 1, and the integration of the additional equation was started at $x = -0.45 \text{ m}$ with the solution of case 1, namely, $r = s$. The resulting $\delta(x)$ are also shown in Fig. 1. In this case singularities occur for $A < -19.9$, but $\delta(x)$ is quite different from case 1 as the upstream history of w_1 is now taken into account.

Finite-Difference Code: Case 3

Bettellini's² finite-difference code was used by D. Gasser to calculate the flow shown in Fig. 2 for a laminar boundary layer. The results are fairly similar to those of case 2 but the parameter A is quite different. Singularities ("floating overflow") were observed for $A < -12$. Computations for turbulent flow were based on the turbulence model described by Pompeo et al.¹ and indicated divergence for $A < -30$. The location of the singularity predicted with the different methods is also shown in Fig. 2. It shows that singularities occur for sufficiently strong convergence (sufficiently negative A) independent of the method used.

Conclusion

Families of boundary layers converging toward a plane of symmetry were investigated. The external axial velocity in the plane of symmetry was assumed to be constant. Therefore, no pressure gradient could decelerate the axial flow. In spite of this singularities with excessive boundary-layer thickness and vanishing skin friction were encountered for sufficiently strong convergence of the outer flow toward the plane of symmetry. This singularity, caused by the boundary-layer assumptions, can also generate unexpected problems in more complicated calculations of three-dimensional boundary layers. It has not occurred in calculations based on the full Navier-Stokes equations, and it was not observed in the experiments.

References

- Pompeo, L., Bettellini, M. S. G., and Thomann, H., "Laterally Strained Turbulent Boundary Layers near a Plane of Symmetry," *Journal of Fluid Mechanics*, Vol. 257, Dec. 1993, pp. 507-532.
- Bettellini, M. S. G., "Numerical Study of Some Engineering Turbulence Models for Three-Dimensional Boundary Layers," Dissertation No. 9182, Swiss Federal Institute of Technology, Zurich, Switzerland, 1990.
- Eichelbrenner, E. A., "Three-Dimensional Boundary Layers," *Annual Review of Fluid Mechanics*, Vol. 5, 1973, pp. 339-360.
- Moore, F. K., "Three-Dimensional Boundary Layer Theory," *Advances in Applied Mechanics*, Vol. IV, 1956, pp. 159-228.
- Boericke, R. R., "Laminar Boundary Layer on a Cone at Incidence in Supersonic Flow," *AIAA Journal*, Vol. 9, No. 3, 1971, pp. 462-468.
- Der, J., "A Study of General Three-Dimensional Boundary-Layer Problems by an Exact Numerical Method," *AIAA Journal*, Vol. 9, No. 7, 1971, pp. 1294-1302.
- Brown, S. N., and Stewartson, K., "Laminar Separation," *Annual Re-*

view of *Fluid Mechanics*, Vol. 1, 1969, pp. 45–72.

⁸Williams, J. C., "Incompressible Boundary-Layer Separation," *Annual Review of Fluid Mechanics*, Vol. 9, 1977, pp. 113–144.

⁹Cousteix, J., "Three-Dimensional and Unsteady Boundary Layer Computations," *Annual Review of Fluid Mechanics*, Vol. 18, 1986, pp. 173–196.

¹⁰Schlichting, H., *Grenzschicht-Theorie*, G. Braun, Karlsruhe, Germany, 1982, pp. 160, 208.

Performance of the k - ϵ Model in Computation of Asymmetric Turbulent Near Wakes

S. Vengadesan* and A. Nakayama†
Kobe University, Kobe 657, Japan

Introduction

PERFORMANCE of the k - ϵ turbulence model as used to compute two-dimensional turbulent wakes has been examined by calculating symmetric and asymmetric wakes in nominally zero-pressure gradients in the absence of such complicating parameters as pressure gradient and curvature. Wakes with small asymmetry are computed accurately, but the accuracy diminishes for strong asymmetry even in the near wake region. It is found that it is due to increasing importance of the turbulent transports in strongly asymmetric flows, which the k - ϵ model does not represent well, particularly the counter-gradient diffusion found in strongly asymmetric wake flows.

Calculation Method and Test Cases

The standard k - ϵ method of Launder and Spalding¹ with the standard values of constants has been used to assess its performance. In the present test cases, the pressure variation is small and can be considered to be given; hence, a parabolic method is used starting the calculation at the trailing edge of the wake-producing model. The initial conditions are taken from the experimentally

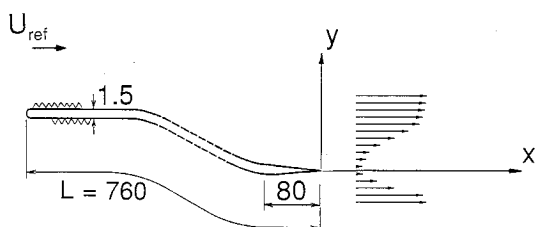


Fig. 1 Configuration of test flows.

Table 1 Characteristics of the test flows at $x = 0$

	Symmetric, mm	Case A, mm	Case B, mm	Case C, mm
δ_{995} , upper side	20	60	34	88
δ_{995} , lower side	20	12	25	15
θ_t	4.7	6.8	5.0	11.3
C_f , upper side	0.0035	0.0033	0.0043	0.0027
C_f , lower side	0.0036	0.0034	0.0030	0.0038
Re_θ , upper side	1840	7420	4200	13800
Re_θ , lower side	1840	1647	3300	1210

Received Jan. 26, 1993; revision received Feb. 28, 1994; accepted for publication March 12, 1994. Copyright © 1994 by the American Institute of Aeronautics and Astronautics, Inc. All rights reserved.

*Research Student; currently Graduate Assistant, Mechanical Engineering Department, West Virginia University, Morgantown, WV 26505.

†Associate Professor, Faculty of Engineering, Rokkoda, Nada-Ku, Associate Fellow AIAA.

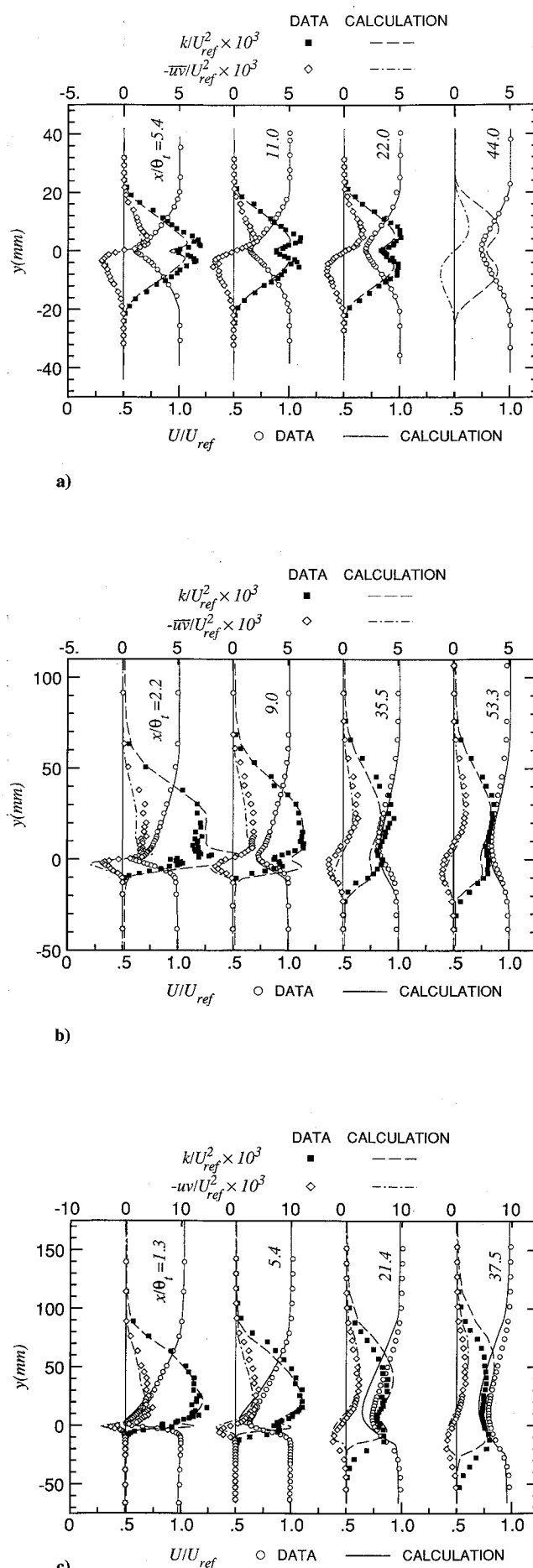


Fig. 2 Comparison of calculation and experimental data: a) symmetric wake, b) asymmetric wake case A, and c) asymmetric wake case C.